

MIMO OFDM Chirp Waveform Design With Spread Spectrum Modulation

Sheng-juan Cheng, Wen-Qin Wang, *Member, IEEE*, and Huaizong Shao

School of Communication and Information Engineering

University of Electronic Science and Technology of China, Chengdu, 611731

Email: shengjuancheng@gmail.com; wqwang@uestc.edu.cn; hzshao@uestc.edu.cn

Abstract—This paper proposes an approach to design orthogonal multiplexing waveform for use of Multiple-input Multiple-output (MIMO) radar. The designed scheme incorporate direct sequence spread spectrum (DSSS) coding techniques on orthogonal frequency division multiplexing (OFDM) chirp signaling. We call it spread spectrum coded OFDM chirp (SSCOC) signaling. The performance of the signals are analyzed with the cross-ambiguity function. In the experiment, the influence of spread spectrum code length and type as well as the bandwidth and duration of OFDM chirp waveforms on cross-ambiguity function (CAF) is discussed. It is verified that the proposed design scheme can ensure these waveforms stay orthogonal on receive and obtain large time-bandwidth product which are beneficial to separate closely spaced targets with ultra-high resolution.

Index Terms—Multiple-input Multiple-output (MIMO), Orthogonal frequency division multiplexing (OFDM), Direct Sequence Spread Spectrum (DSSS), Spread Spectrum Coded OFDM Chirp (SSCOC), Cross-Ambiguity Function (CAF)

I. INTRODUCTION

Multiple-input multiple-output (MIMO) radar is a next-generation radar technique, which employs multiple transmit and receive apertures, equipped with the capability of transmitting arbitrary and diverse signals at each transmit aperture. The added flexibility of individual signal selection at each aperture brings with it the promise of enormous performance improvements and the challenge of finding solutions to extremely high-dimensional optimization problems associated with choosing the right signals. As a consequence, MIMO synthetic aperture radar (SAR) has gained great popularity and attracted much attention in recent years [1]–[4]. However, the waveform design for multiple transmitters has been the most important and challenging issue in realizing MIMO SAR concept.

To address the MIMO radar waveforms design issue, numerous techniques such as employing polarization diverse waveforms [5], frequency diverse waveforms [6], coded waveforms [7], and combination of these methods are proposed [8]. Moran [9] presented polarization diverse waveforms on multiple channels for MIMO radar which enables detection of smaller radar cross section targets and diversity gains. Gladkova [10] described a family of stepped frequency waveforms to attain high range resolution. Many existing methods are based on the assumption that the waveforms stay orthogonal at receiver under the Doppler shifts caused by the motion of targets in a MIMO radar setting [11]. An approach is proposed in [12]

for designing diversity radar waveforms that are orthogonal on both transmit and receive. It incorporates the Walsh-Hadamard code and chirp signal to design two orthogonal waveforms. J. Kim [13] proposes a novel OFDM Chirp waveform design scheme, but only two orthogonal waveforms are designed.

This paper proposes a waveform diversity design scheme based on the OFDM chirp waveform [13] and spread spectrum sequence. The use of OFDM signal in radar systems was proposed firstly in 2000 [14]. The primary disadvantage of using OFDM in wireless communication lies in that time and frequency synchronization is crucial to ensure subcarrier orthogonality; however, sensitivity to time and frequency synchronization is beneficial for radar systems because radar receiver usually uses a stored version of the transmit signal to measure the time-delay and frequency offset between the transmitted and received signals to derive the target parameters [15]–[17]. For these reasons, OFDM SAR has received considerable attention in recent years [18], [19].

On the other hand, spread spectrum sequences are widely used in wireless communications. The transmitted waveforms are rendered orthogonal with a unique spread spectrum code, the echo signal will be decoded using its spreading code. In this manner, transmitted orthogonal waveforms can be match filtered only with the intended received signal. Walsh-Hadamard code, m sequences, GOLD sequences and orthogonal GOLD sequences are usually applied in spread spectrum system. More importantly, spread spectrum sequences perform very well in high interference environment. Therefore, it is necessary to further improve the OFDM chirp waveform orthogonality with spread spectrum sequences.

The remaining sections are organized as follows. Section II introduces the basic four OFDM chirp waveform scheme. Section III presents coded OFDM chirp waveform design based on direct sequence spread spectrum (DSSS) technique. Next, performance analysis is provided in section IV. Finally, this paper is concluded in section V.

II. OFDM CHIRP WAVEFORM DESIGN SCHEME

Kim [13] designed a novel OFDM chirp waveform scheme for use of multiple transmitters in SAR. However, this method offers only two orthogonal signals. To overcome this disadvantage, we extend this method to design four OFDM chirp signals in this section.

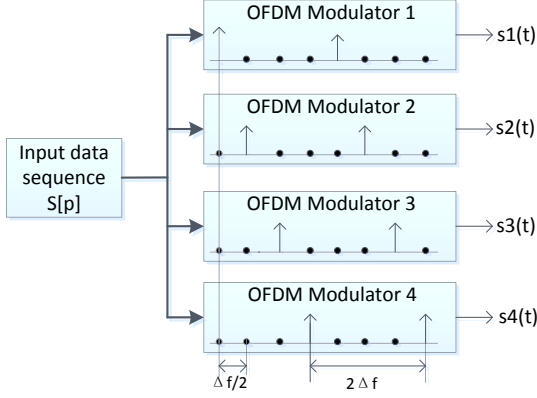


Fig. 1: Four orthogonal OFDM chirp waveforms generate scheme.

Supposing the input sequence $S[p]$ with N discrete spectral components, which are separated by $2\Delta f$. As shown in Figure 1, the input data sequence $S[p]$ is interleaved by $3N$ zeros yields $S_1[p]$. Then, the interleaved data sequence is shift by $\Delta f/2, \Delta f, 3\Delta f/2$ respectively for the second, third, fourth data sequence $S_2[p], S_3[p]$ and $S_4[p]$. Using the $4N$ -point inverse discrete Fourier transform (IDFT), the input data sequences can be transformed into time domain. In doing so, we obtain four waveforms modulated by four orthogonal subcarrier sets that are mutually shifted by $\Delta f/2$. It must be emphasized that all the sets contain $4N$ subcarriers but use only N subcarriers to carry the input data.

According to the design scheme, a chirp signal is used for the OFDM modulation to achieve the constant envelope. In practical implementation using digital instruments, the discrete time samples are denoted as

$$s[m] = \exp(j\pi k_r(mT_s)^2), \quad m = 0, 1, \dots, N-1 \quad (1)$$

where T_s denotes the sampling interval, and k_r is the chirp rate, which is a ratio between the signal bandwidth B and chirp duration T_p ($k_r = B/T_p$). Using the Fourier transform, the chirp spectrum is given by

$$S[p] = \mathcal{F}\{s[m]\} = \mathcal{F}\{\exp(j\pi k_r(mT_s)^2)\} \quad (2)$$

where \mathcal{F} is the Fourier transform.

According to Figure 1, the time-domain waveform $s_1[n]$ is

$$s_1[n] = \frac{1}{4} \left\{ s[n] \text{rect}\left[\frac{n}{N}\right] + s[n-N] \text{rect}\left[\frac{n-N}{N}\right] + s[n-2N] \text{rect}\left[\frac{n-2N}{N}\right] + s[n-3N] \text{rect}\left[\frac{n-3N}{N}\right] \right\} \quad (3)$$

where $n = 0, 1, \dots, 4N-1$.

As the four orthogonal subcarrier sets are mutually shifted by $\Delta f/2$, the other three waveforms can be derived directly from $s_1[n]$ as follows:

$$s_i[n] = s_1[n] \exp\left(j\frac{(i-1)\pi n}{2N}\right), \quad i = 2, 3, 4. \quad (4)$$

Their continuous time representations are expressed, respectively, as

$$s_1(t) = \frac{1}{4} \left\{ s(t) \text{rect}\left[\frac{t}{T_p}\right] + s(t-T_p) \text{rect}\left[\frac{t-T_p}{T_p}\right] + s(t-2T_p) \text{rect}\left[\frac{t-2T_p}{T_p}\right] + s(t-3T_p) \text{rect}\left[\frac{t-3T_p}{T_p}\right] \right\} \quad (5)$$

$$s_i(t) = s_1(t) \exp\left(j\pi \frac{it}{4T_p}\right), \quad i = 2, 3, 4. \quad (6)$$

III. SPREAD SPECTRUM CODED OFDM CHIRP WAVEFORM DESIGN

In this section, we design the waveform diversity by integrating spread spectrum code into the four OFDM chirp signals. We call it spread spectrum coded OFDM chirp (SSCOC) signaling.

For simplicity and without loss of generality, we take the OFDM chirp signal $s_1(t)$ and $s_2(t)$ as original input data to design the SSCOC waveforms.

First define two direct sequence spread-spectrum coded OFDM chirp signals as follows:

$$sc_1(t) = \sum_m^{M-1} C_m P(t - mT_c) s_1(t) \quad (7)$$

$$sc_2(t) = \sum_n^{M-1} D_n P(t - nT_c) s_2(t) \quad (8)$$

where

C_m, D_n : the first and second code sequence respectively

T_p : chip time

$P(t)$: rectangular pulse

To further see what happens when the targets are moving, we correlate the emitted pulse with a copy shifted in range and Doppler shift. This can be evaluated by the cross-ambiguity function between $sc_1(t)$ and $sc_2(t)$ [20]

$$\begin{aligned} \chi_{sc_1, sc_2}(\tau, f_d) &= \int_R sc_1(t) sc_2^*(t-\tau) e^{j2\pi f_d t} dt \\ &= \int_R \left(\sum_m^{M-1} C_m P(t - mT_c) s_1(t) \right) dt \\ &\quad \left(\sum_n^{M-1} D_n P(t - nT_c - \tau) s_2(t - \tau) \right)^* e^{j2\pi f_d t} dt \\ &= \sum_m^{M-1} \sum_n^{M-1} C_m D_n^* \\ &\quad \int_R P(t - mT_c) s_1(t) P(t - nT_c - \tau) s_2(t - \tau)^* e^{j2\pi f_d t} dt \end{aligned} \quad (9)$$

where f_d is the Doppler shift, τ is the delay time. Specially, when $sc_1(t) = sc_2(t)$ it simplifies to the self-ambiguity function. This ambiguity function evaluated at $(\tau, f_d) = (0, 0)$ is equal to the matched filtering output that is matched perfectly to the signal reflected from the target of interest.

From equation (9) above, some important properties of the SSCOC signals can be guessed as following:

1) The type of spread spectrum code such as Walsh-Hadamard code, GOLD sequence etc. will influence the auto and cross-ambiguity response.

2) The code length such as 4, 8, 16, 32 or 64 will also determine the degree of orthogonality of the received signal. Furthermore, the code length will influence the bandwidth expansion of the coded signals.

3) The duration T_p and bandwidth B will make some contributions to the cross-ambiguity function.

All the properties will be verified in Section IV.

IV. EXPERIMENTS ON PERFORMANCE OF SSCOC SIGNALING

We investigate the proposed SSCOC signaling and examined the auto-ambiguity and cross-ambiguity responses. Table I gives the simulation parameters. The final bandwidth BW of the designed SSCOC waveform is determined by

$$BW = B_{equal} \left(\frac{1}{T_p} + \frac{1}{T_c} \right) \quad (10)$$

where $T_c = T_p/NC$ and B_{equal} is a factor of the same value with original bandwidth B .

In the following, we analyze the influence of pulse code length NC , code type, original bandwidth B and pulse duration T_p to cross-ambiguity function, respectively. Note that the cross-ambiguity response is normalized by the auto-ambiguity peak to compare their difference clearly.

TABLE I: Experimental parameters of OFDM chirp signals

Parameters	Values
Bandwidth (B)	4 MHz
Pulse Duration (T_p)	1 μs
Pulse Chirp Rate (K_r)	B/T_p
Pulse Code Length (NC)	2^m or $2^m - 1$ ($m=2,3,4,5,6,7$)

A. Pulse Code Length Impact Analysis

The pulse code length determines the bandwidth of the coded signal and has an influence on the cross-ambiguity response. For simplicity and without loss of generality, Walsh-Hadamard code is used in the experiment to compare the cross-ambiguity response with different code lengths. The initial bandwidth of 4 MHz has been used for the code length 1 which is the scenario of just using OFDM chirp signal without any spectrum coding. According to (10), bandwidths of 20 MHz, 36 MHz, 68MHz, 132 MHz, 260 MHz and 516 MHz correspond to the code lengths of 4, 8, 16, 32, 64 and 128, respectively. Table II gives the comparative results. Obviously, for a given code, the longer it is, the better cross-ambiguity response it gains. For the code lengths of 1 and 8, the maximum cross-ambiguity values observed are about 0.9988 and 0.7234, respectively. Similarly, using longer code length of 16, 32, 64, 128, improved cross-ambiguity responses are obtained. It can be concluded that the cross-ambiguity peak will be smaller with increased code length, namely the degree of orthogonality will improved.

B. Code Type Property Discussion

The code types such as Walsh-Hadamard code, m sequence, Gold code, orthogonal GOLD code etc. will influence the cross-ambiguity and auto-ambiguity response (i.e. degree of

TABLE II: Performance of SSCOC signals with different length

code type	code length	bandwidth(MHz)	max AAF	max CAF
-	1	4	1	0.9988
Walsh	4	20	1	0.7234
Walsh	8	36	1	0.6649
Walsh	16	68	1	0.5551
Walsh	32	132	1	0.4887
Walsh	64	260	1	0.4196
Walsh	128	516	1	0.3649

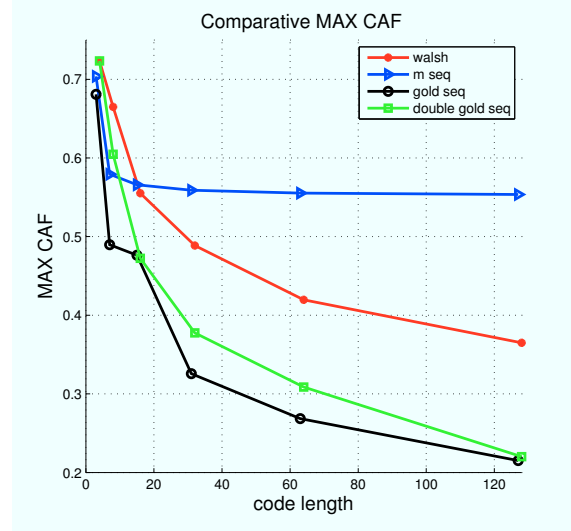


Fig. 2: Comparative MAX CAF among Different Types.

orthogonality of the received signal). Here, the effect of Walsh-Hadamard code, m sequence, Gold sequence and orthogonal GOLD sequence on the SSCOC waveforms are discussed. For Walsh-Hadamard code and orthogonal GOLD sequence, the code lengths are 2^l ($l = 2, 3, 4, 5, 6, 7$). While the length of $2^l - 1$ is used for the m and Gold sequences. Figure 2 shows comparative CAF response using different code types. It is obvious that the degree of orthogonality is best for the GOLD sequence. The maximum cross-ambiguity response observed is about 0.2 with the code length of 127. However, the cross-ambiguity peak has little variation for the m sequence. Take both bandwidth and degree of orthogonality into consideration, GOLD code is the best suitable code to apply in SSCOC signaling and orthogonal GOLD sequence is the second one. It can be estimated that if we want to obtain lower cross-ambiguity peak, a longer code length can be employed.

C. Bandwidth Reduction Property of SSCOC Signaling

From TABLE II, we can see that bandwidth expansion will be greater with the increased code length. In practical application, the bandwidth is a scarce resource. In particular, using bandwidth more than 1GHz could be expensive for hardware implementation. To analyze the bandwidth reduction problem, we set the bandwidth with 0.01 MHz, 0.1 MHz, 1 MHz, 4 MHz, 20 MHz and 1000 MHz, while pulse duration T_p is 1 μs , code type is Walsh-Hadamard code

and the length of code is 64. Table III gives that the CAF response almost has no impacts on the increased bandwidth and orthogonality of signals. Therefore we can reduce the initial bandwidth to gain equivalent degree of orthogonality by a large factor. It is an important property of the SSCOC signaling.

TABLE III: Bandwidth reduction property of SSCOC signaling

Code type	Code length	Bandwidth(MHz)	Max AAF	Max CAF
-	64	0.01	1	0.4196
Walsh	64	0.1	1	0.4196
Walsh	64	1	1	0.4259
Walsh	64	4	1	0.4196
Walsh	64	20	1	0.4196
Walsh	64	100	1	0.4196
Walsh	64	1000	1	0.4196

D. The Influence of Duration on CAF Response

High chirp rate demands high performance hardware device. Since bandwidth almost has no influence on the CAF response, we can enlarge the duration T_p to reduce the chirp rate K_r . In the simulation, the duration sets are 0.001 μs , 0.1 μs , 0.01 μs , 1 μs , 10 μs , 100 μs and 1000 μs while bandwidth is 4 MHz, code type is the Walsh-Hadamard code with a code length of 64. Table IV shows different durations produce nearly identical degree of orthogonality. This property is useful to reduce demand for hardware devices.

TABLE IV: Pulse duration influence on CAF response

Code type	Code length	Duration(μs)	Max AAF	Max CAF
-	64	0.001	1	0.4196
Walsh	64	0.01	1	0.4196
Walsh	64	0.1	1	0.4196
Walsh	64	1	1	0.4196
Walsh	64	10	1	0.4196
Walsh	64	100	1	0.4256
Walsh	64	1000	1	0.4196

V. CONCLUSION

In this paper, a method is proposed to design spread spectrum coded OFDM chirp waveforms by combing the OFDM chirp waveform and direct sequence spread spectrum technique. Simulation results show that the proposed method can maintain the orthogonality of the received waveforms effectively. The contributions are summarized as: 1) The GOLD sequence is the best suitable code to reduce the cross-ambiguity peak. 2) The bandwidth and duration have little influence on the cross-ambiguity response. 3) This waveform inherits Doppler tolerant and auto-correlation property of OFDM chirp waveforms when properly processed. In subsequent work, we plan to further analyze performance of this waveform in a noisy environment.

ACKNOWLEDGEMENTS

The work described in this letter was supported in by the National Natural Science Foundation of China under grant 41101317, the Program for New Century Excellent Talents in

University under grant NCET-12-0095 and Sichuan Province Science Fund for Distinguished Young Scholars under grant 2013JQ0003.

REFERENCES

- [1] D. Cerutti-Maori, I. Sikaneta, J. Klare, and C. H. Gierull, "MIMO SAR processing for multichannel high-resolution wide-swath radars," *IEEE Transactions on Geoscience and Remote Sensing*, vol. 55, pp. 1–22, 2014, doi:10.1109/TGRS.2013.2286520.
- [2] W.-Q. Wang, "MIMO SAR imaging: Potential and challenges," *IEEE Aerospace and Electronic Systems Magazine*, vol. 27, no. 8, pp. 18–23, August 2013.
- [3] D. Tarchi, F. Oliveri, and P. F. Sammartino, "MIMO radar and ground-based SAR imaging systems: equivalent approaches for remote sensing," *IEEE Transactions on Geoscience and Remote Sensing*, vol. 51, no. 1, pp. 425–435, January 2013.
- [4] W.-Q. Wang, "Large-area remote sensing in high-altitude high-speed platform using MIMO SAR," *IEEE Journal of Selected Topics in Applied Earth Observation and Remote Sensing*, vol. 6, no. 5, pp. 2146–2158, October 2013.
- [5] R. Calderbank, S. Howard and B. Moran, "Waveform Diversity in Radar Signal Processing," *IEEE Signal Processing Magazine*, vol. 26, no. 1, pp. 32–41, Jan. 2009.
- [6] J. M. de Wit, W. L. Van Rossum and A. J. De Jong, "Orthogonal Waveforms for FMCW MIMO Radar," *IEEE Radar 2011*, pp. 686–691, 2011.
- [7] S. R. J. Axelsson, "Suppressed Ambiguity in Range by Phase-Coded Waveforms," *Processing of the IEEE 2001 Geoscience and Remote Sensing Symposium (IGARSS 01E)*, vol. 5, pp. 2006–2009, 2001.
- [8] C.-F. Chang and M. R. Bell, "Frequency-Coded Waveforms for Enhanced Delay-Doppler Resolution," *IEEE Transactions on Information Theory*, vol. 49, no. 11, pp. 2060–2071, Nov. 2003.
- [9] S. Howard, A. Calderbank and W. Moran, "A Simple Signal Processing Architecture for Instantaneous Radar Polarimetry," *IEEE Transactions on Information Theory*, 2007, vol. 53, no. 4, pp. 1282–1289, April 2007.
- [10] I. Gladkova, "Analysis of Stepped-Frequency Pulse Train Design," *IEEE Transactions on Aerospace and Electronic Systems*, vol. 45, no. 4, pp. 1251–1261, Oct. 2009.
- [11] B. Friedlander, "On the Relationship Between MIMO and SIMO Radars," *IEEE Transactions on Signal Processing*, vol. 57, no. 1, pp. 394–398, Jan. 2009.
- [12] K. Majumder, R. Mark, "A Novel Approach for Designing Diversity Radar Waveforms that are Orthogonal on Both Transmit and Receive," *Processing of IEEE Radar Conference*, 978-1-4673-5794-4, 2013.
- [13] J. H. Kim, Marwan Younis, Alberto Moreira, "A novel OFDM chirp waveform scheme for use of multiple transmitter in SAR," *IEEE Transactions Geoscience Remote Sensing*, vol. 10, no. 3, pp. 658–572 May. 2013.
- [14] N. Levenon, "Multi frequency complementary phase-coded radar signal," *IET Radar Sonar Navigation*, vol. 147, no. 6, pp. 272–284, Dec. 2000.
- [15] D. R. Fuhrmann, J. P. Browning and M. Rangaswamy., "Signaling strategies for the hybrid MIMO phased-array radar," *IEEE Journal of Selected Topics in Signal Processing*, vol. 4, no. 1, pp. 66–78, Feb. 2010.
- [16] D. Garmatyuk, J. Schuerger, K. Kauffman, S. Spalding, "Wideband OFDM system for radar and communications," *Processing of IEEE Radar Conference*, Pasadena, CA, pp. 1–6, May 2009.
- [17] W.-Q. Wang, *Multi-Antenna Synthetic Aperture Radar*. New York: CRC Press, May 2013.
- [18] W.-Q. Wang, "Space-time coding MIMO-OFDM SAR for high-resolution remote sensing," *IEEE Transactions on Remote Sensing*, vol. 49, no. 8, pp.
- [19] G. Krieger, M. Younis, S. Huber, "MIMO-SAR and orthogonality confusion," *Transactions Geoscience Remote Sensing*, pp. 1533–1536, 2012.
- [20] H. Yan ,G. Shen, R. Zetik, O. Hirsch and R. S. Thoma, "Ultra-Wideband MIMO Ambiguity Function and Its Factorability," *Transactions Geoscience Remote Sensing*, vol. 51, no. 1, pp. 504–518, Jan. 2013.